

NEUTRON DIFFRACTION AND EPSR SIMULATIONS OF THE HYDRATION STRUCTURE AROUND PROPANE MOLECULES BEFORE AND DURING GAS HYDRATE FORMATION

¹N. H. Aldiwan, ¹Y. Lui, ²A.K. Soper, ²H. Thompson, ³J.L. Creek,

⁴R.E. Westacott, ⁵E.D. Sloan, ^{5*}C.A. Koh

¹King's College London, Strand, London, WC2R 2LS, U. K.

²ISIS Facility, Rutherford Appleton Laboratory, OXON, OX11 0QX, U.K.

³ChevronTexaco Energy Technology Company, Houston, TX 77082, U.S.A.

⁴Heriot-Watt University, Chemical Engineering Dept., Edinburgh, EH14 4AS, U.K.

⁵Colorado School of Mines, Center for Hydrate Research, Golden, CO 80401, U.S.A.

ABSTRACT

Fundamental understanding of the structural changes occurring during hydrate formation and inhibition is important in the development of new strategies to control hydrates in flowlines and in inhibitor design. Neutron diffraction coupled with Empirical Potential Structure Refinement (EPSR) simulation has been used to determine the hydration structure around propane molecules before and during sII hydrate formation. The EPSR simulation results were generated by fitting neutron data (with H/D isotopic substitution) obtained from the SANDALS diffractometer at ISIS. Using this combination of techniques, the structural transformations of water around propane can be studied during propane (sII) hydrate formation. The hydration structure was found to be different in the liquid phases of the partially formed propane hydrate compared to that before any hydrate formation. The effect of a kinetic hydrate inhibitor, poly-N-pyrrolidone on the hydration structure was also examined. No significant effect was observed on the water structure in the presence of this inhibitor.

Keywords: gas hydrates, neutron diffraction, kinetic inhibitors

INTRODUCTION

Investigations aimed directly at understanding the hydration structure during hydrate formation are important in providing experimental verification for the mechanism(s) proposed for hydrate formation [1]. Presented in this paper are the findings from first order H/D isotope substitution neutron diffraction experiments performed on a propane-water system aimed at directly probing the water structure before and during propane

hydrate formation. Also presented are EPSR simulations of the liquid phases of the part-formed stages of propane hydrate. Molecular modelling of the propane hydrate crystal is presented for comparison.

Insights into the effects of kinetic inhibitors on the gas hydrate former-water hydration structure (i.e. before any hydrate forms) would have direct relevance to the gas industry. This is because propane forms sII type hydrate, which is the same

hydrate structure that is typically formed by natural gas in pipelines. The effect of the kinetic inhibitor PVP was tested in a separate set of neutron diffraction experiments. The water structure in the presence of PVP was examined from the total structure factors obtained from these experiments. The findings from these experiments along with comparisons with propane hydrate melt containing no inhibitor are also presented for comparison.

METHODS

Neutron Diffraction Experiments

The hydration structure around propane was measured using the time-of-flight SANDALS (small angle neutron diffractometer for amorphous and liquid samples) diffractometer at the ISIS facility. SANDALS was chosen because the detector banks are positioned at relatively small angles ($<40^\circ$) which helps to minimise the effects of the inelastic neutron scattering on the diffraction pattern from protiated samples [2].

Protiated and deuteriated propane gas (C_3H_8 and C_3D_8 , respectively) was added to D_2O in order to follow propane hydrate formation. The isotope substitutions were made on the propane gas rather than water hydrogens since the aim was to follow hydrate formation through measuring the structure of water around the propane atoms. The two isotopically substituted but otherwise identical samples were contained in a Ti-Zr specially designed high pressure cylindrical reactor cell.

The propane-water mixtures (8 ml) were thoroughly mixed inside the pressure cell by a pneumatic agitator that continually inverted the cell by 90° . For each of the two samples the water and gas were mixed inside the cell for 2 hrs prior to any diffraction measurements. The temperature of the sample was maintained by circulating refrigerated water from a cooling bath around the sample. See [3] for further details of the sample cell configuration.

The samples were initially frozen to seed the formation from ice. To form propane hydrate the propane-water/ice mixture was held at a pressure of 7 bar and the temperature was increased to $6^\circ C$. Hydrate growth was followed by monitoring the Bragg peaks in the measured total structure factors, i.e. the $F(Q)$ for the samples. Neutron

diffraction measurements were taken during the formation stages until these Bragg peaks ceased to grow and there was no further propane gas consumption by the sample. At this temperature and pressure the propane-water mixture was $0.5^\circ C$ below the required temperature to form propane hydrate.

The experiments were repeated, but with the addition of the hydrate inhibitor PVP to the propane-water liquid mixture prior to any hydrate formation. 1 wt % PVP was added to each of the protiated ($C_3H_8 + D_2O + PVP$) and deuteriated ($C_3D_8 + D_2O + PVP$) propane-water samples.

The raw neutron diffraction data collected were then corrected using standard procedures. Information on all aspects of these corrections can be found in the ATLAS manual [2]. For each experiment two total structure factors were obtained, each one corresponding to one of the two solutions prepared (either protiated or deuteriated). These total structure factors are a linear combination of several weighted partial structure factors, $S(Q)$, with the weights being a product of the scattering length and relative concentration of each atomic species.

General Neutron Diffraction Data Analysis

The total structure factors, $F(Q)$ s, (differential cross sections minus the self-scattering) obtained in this experiment contain information about the ten intermolecular correlations that exist in the sample. These are the C-C, C-M, C-Ow, C-Hw, M-M, M-Ow, M-Hw, Ow-Ow, Ow-Hw and the Hw-Hw correlation, where C is propyl carbon, M is propyl hydrogen, Ow is water oxygen and Hw is water hydrogen.

The first order difference is obtained by subtracting the C_3H_8/D_2O diffraction pattern from the one obtained for the C_3D_8/D_2O sample. The resulting diffraction pattern is thus dominated by the substituted species and hence is especially sensitive to the distribution of water around propane. The first order difference contains only correlations involving propyl-hydrogens, since any correlations not involving these hydrogen atoms will cancel out.

Diffraction data were obtained for the initial propane-water mixture, i.e. 0% hydrate formed.

Data were also obtained for the 6%, 10% and 20% formed (% hydrate converted from water/gas). The maximum amount of propane hydrate formed was ~20% for the samples investigated.

The degree of crystallinity for each set of data, $F(Q)_{\text{part-formed}}$, was determined by subtracting various percentages of the initial propane-water amorphous data (i.e. 0% formed hydrate) from the specific $F(Q)$ s for the formation stages. The actual percentage of hydrate formation (conversion) in each sample is thus determined by how much 0% formed mixture has to be subtracted from this data, i.e. subtracting all the amorphous background and leaving behind only the crystalline structure. Written in equation form this can be simplified as follows:

$$F(Q)_{\text{crystalline structure}} = \frac{[F(Q)_{\text{part-formed}} - x(0\% \text{ formed})]}{(1 - x)},$$

where x is the fraction of the amorphous background in each data set.

A correlation between the percentage of propane hydrate formed and the increase in Bragg (sharp) peaks in each total structure factor (which reflects this increased crystallization of the sample) can be seen in figures 1 and 2. These total structure factors contain amorphous background structural information, but as the amount of hydrate in the sample grows the contribution from the crystalline structure becomes greater. In both figures there is a consistent pattern of Bragg peak growth with increased percentage of formation, as should be expected. Additionally, in both figures the total structure factor for the 0% hydrate formed shows no Bragg peaks and just the amorphous background.

On comparing the general shape of the differential cross sections obtained from the protiated and deuteriated propane samples, sharper Bragg peaks are observed in the sample from protiated propane with some of these peaks not featuring in the diffraction pattern of the deuteriated sample. This is due to the large difference in positive scattering length of deuterium in deuteriated water and the negative scattering of hydrogen in protiated propane.

Molecular Modeling: The EPSR Technique

The empirical potential structure refinement (EPSR) technique has been used to model a

variety of amorphous systems [4,5]. However, the fact that EPSR was not built to model amorphous and crystalline data in the same simulation box means that the only way to simulate the data from the part-formed stages (which contains both amorphous and crystalline structure) was to separate the crystal and liquid data in order to perform independent simulations of each.

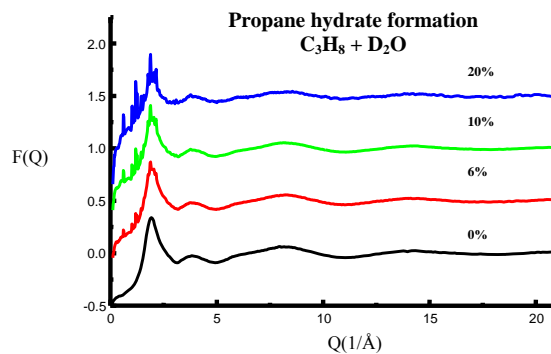


Figure 1. The total structure factors for the propane hydrate formation stages at 0%, 6%, 10% and 20% (maximum formed) obtained from the protiated propane hydrate experiment, $C_3H_8 + D_2O$

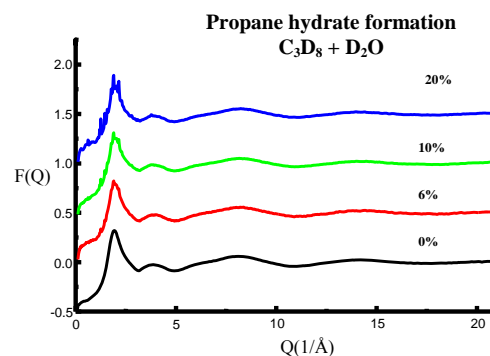


Figure 2. The total structure factors for the propane hydrate formation stages at 0%, 6%, 10% and 20% (maximum formed) obtained from the deuteriated propane hydrate experiment, $C_3D_8 + D_2O$

A further challenge was attempting to model the propane hydrate data where the maximum amount of hydrate formed was only 20%. Effectively this meant that the total structure factor, $F(Q)$, containing this 20% hydrate formation also contained 80% underlying amorphous structure (water and propane gas that has not converted to hydrate). Hence, a purely crystalline dataset for the propane hydrate crystal had to be recreated. This was done by subtracting 0.8 times the data set for

0% propane-water (i.e. propane-water liquid with no hydrate) from the 20% formed propane hydrate data set and renormalizing. This left only the crystalline part of the total structure factor in the measured differential cross-section. This recreated propane hydrate fully formed crystal data, as shown in figure 3a for the protiated propane hydrate crystal ($C_3H_8 + D_2O$) and in figure 3b for the deuteriated propane hydrate crystal ($C_3D_8 + D_2O$). These total structure factors are the 20% (maximum) formed data minus the amorphous background for each total structure factor.

Hence, crystal $F(Q)$

$$= (\text{total } F(Q) - (1-x)[0\% \text{ formed liquid } F(Q)]) / x$$

where x is the degree of crystallinity.

Hydrate Crystal Simulations

For the propane hydrate crystal simulation the initial atomic coordinates of the system were derived from sII hydrate crystal X-ray diffraction data [6]. It is only the large cages in the hydrate that have been assumed to be occupied by propane molecules. The simulation box used was a cube of length 69.2\AA . This relatively large box size was necessary in order to allow the maximum resolution for calculating the simulated Bragg peaks. The atomic positions were then allowed to relax during the course of the simulation, but not to any large extent that would cause the structure to become disordered or even ‘melt’ resulting in a purely amorphous sample. This first step would necessarily result in the crystal structure becoming slightly disordered at first, but as evident from the EPSR generated radial distribution functions (which show long range order) the crystal structure was well maintained by the simulation. This was achieved by limiting the step size for the translation of the molecules, such that the EPSR simulation was unable to overcome the energy barrier required to ‘melt’ the simulated hydrate structure.

There is a difference in peak amplitude between the measured and diffraction data in the propane hydrate crystal $F(Q)$ s presented in figure 3 which is related to resolution, but essentially the EPSR Bragg peaks are largely preserved in shape and position. The EPSR technique had been shown, as in our previous studies [7], to be able to fit crystalline structure and not just amorphous data by the good fits (provided changes to the simulation procedure are made by limiting the translational step size).

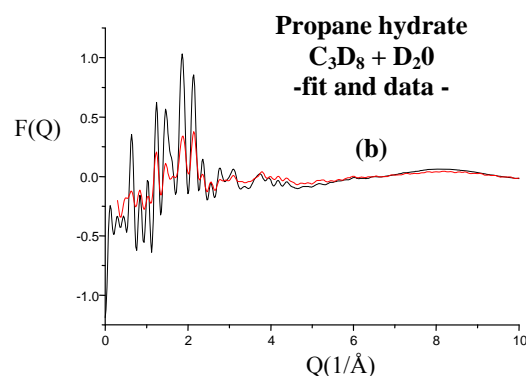
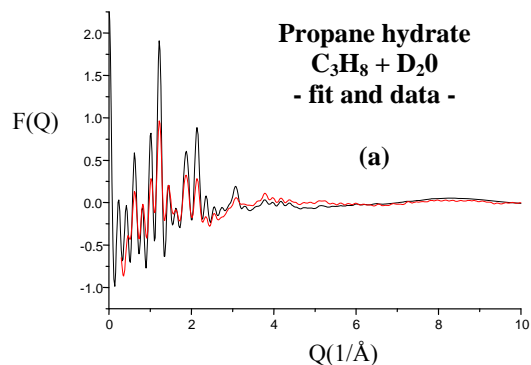


Figure 3. The extracted total structure factors for the propane hydrate crystal: (a) $C_3H_8 + D_2O$, (b) $C_3D_8 + D_2O$. The EPSR determined (fit) to the measured structure factors is shown in red

Amorphous Data Analysis

The neutron diffraction measurements on the 0% formed propane-water solution were actually taken after the propane-hydrate had decomposed, at a pressure of 7 bar and temperature ranging between $9 - 11^\circ\text{C}$. In order to obtain purely amorphous data to simulate the liquid fraction of the part-formed data, the amorphous part of the part-formed propane hydrate formation stages had to be extracted from the part-formed (6% and 10% formed) total structure factors.

Simulation of the propane-water liquid phase of the part-formed data required that crystalline structure had to be removed from this data leaving only the underlying amorphous structure. This is summarized by a similar equation to the one given for the hydrate crystal. The equation for removing the crystalline structure from the 6% and 10% formed data sets, is given as follows:

Liquid $F(Q) =$
(total $F(Q) - x[\text{fully-formed crystal } F(Q)]/(1-x)$),
where x is the fraction of crystal formed.

These total structure factors from the propane hydrate formation stages, showing only the amorphous structure for the 6% and 10% formed data confirm that that all the Bragg peaks have been successfully subtracted from the data, i.e. there is no crystal structure left in the data.

Analysis of Propane-Water Liquid Phases During Hydrate Formation

The propane-water systems were simulated with EPSR using a concentration of 1 propane molecule for every 100 water molecules in the simulation box. The seed interatomic potentials for this simulation were taken from the Jorgensen *et al.* potential for propane [8] and the SPC/E (simple point charge/extended) potential for water [9]. These potential parameters were applied to all the pairs of atoms in the mixture and the initial site-site potentials were then used to build a model with configurations of molecules that reproduce the diffraction data as closely as possible.

What followed was an execution of the EPSR algorithm on the model. After the system had reached equilibrium, a perturbation to the starting reference potential was derived from the difference between the measured neutron diffraction data and the computer simulated model. This new potential is then fed back into the simulation and iteratively used to run the Monte Carlo simulation in order to generate the structure factors and radial distribution functions for the system.

The fits to the data were in good agreement at the low Q region of each plot, though there was some difficulty in fitting the smaller second peak in each $F(Q)$. This slight deviation in fit is due to the difficulties in accurately correcting for the inelastic neutron scattering. However, this low Q region is representative of large intermolecular distances between different atom types and is of no interest in this study.

The EPSR simulated model of the measured data was used to obtain the partial pair correlation functions, $g(r)$ for the part-formed hydrate cases (6% and 10% formed), propane-water with no

hydrate present (0% formed), and the propane hydrate crystal. The propane-water mixture is dominated by the water-water correlations. This can be explained by the large number of water molecules in the simulation box compared to the number of propane molecules (1 propane molecule to every 100 water molecules in the liquid). The isotope substitution on the propyl-hydrogens makes it possible to gain insight into the water ordering around the dissolved propane molecules. The four correlations that describe the structure of water around the propane molecules are the $g_{C-Ow}(r)$, $g_{C-Hw}(r)$, $g_{M-Ow}(r)$ and $g_{M-Hw}(r)$ functions.

3. RESULTS AND DISCUSSION

Propane-Water Mixture and Liquid Phases During Propane Hydrate Formation

The EPSR determined water-water radial distribution functions obtained from modeling the propane-water mixtures at 0%, 6% and 10% are shown in figure 4(a-c). The first peak corresponding to the first oxygen-oxygen nearest neighbor distance (figure 4a) is largely preserved in position and amplitude and is centered at about 2.74Å. Integration under this peak for the three samples reveals the same coordination number of about 4 molecules for all 3 cases as would be expected for tetrahedral water. The second peak in these correlations shows a decrease in amplitude in going from 0% to the part-formed cases (i.e. 6% and 10%). At 0% formation this peak is centered at about 4.45Å and in the part-formed liquid phases it is shifted to a distance of 4.54Å suggesting that the water structure is different depending on whether there is hydrate in the sample or not. The peak shift (although small) suggests that the hydration shell is slightly expanded in the part-formed cases. The amplitudes of these peaks decrease after the formation of hydrate, giving less tetrahedral ordering than in pure water. Integration under these peaks reveals that in the part-formed cases the oxygen-oxygen coordination number is approximately 1 water molecule less than the case with no hydrate present.

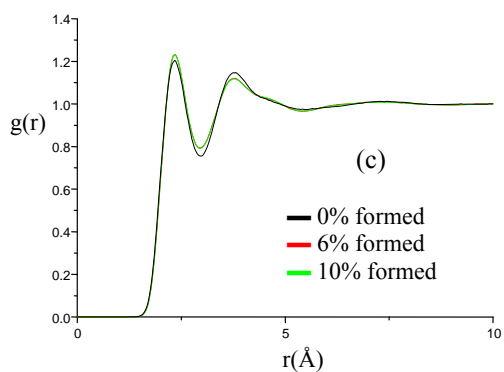
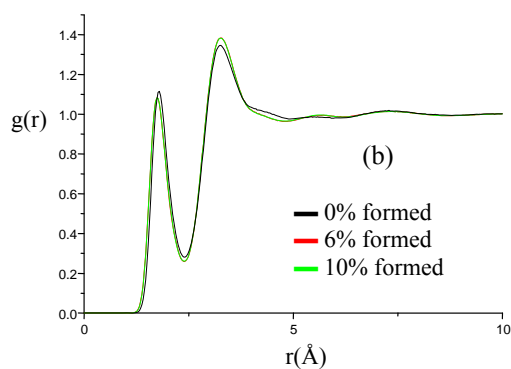
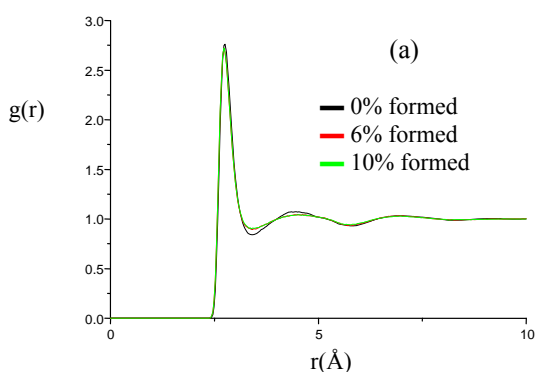


Figure 4. The water-water partial pair correlation functions: (a) $g_{OwOw}(r)$, (b) $g_{OwHw}(r)$, and (c) $g_{HwHw}(r)$ correlations determined by the EPSR procedure from the simulated propane-water model at 0% (black), 6% (red) and 10% (green) propane hydrate formation.

The hydrogen water-hydrogen water correlation (figure 4c) also shows differences in peak amplitudes for the correlations from the 6% and 10% samples compared to the propane-water sample at 0%, where there appears to be a clear decrease in height of the second peak compared to the 0% sample.

The EPSR determined spatial density functions of water molecules around a central propane molecule show this subtle change in the water structure (figure 5). There is little change in the first hydration shell but the most significant change is in the second hydration shell which looks like it is expanding. Since the lobes in the second shell are getting smaller and none of the others increase in size, it can be concluded that water molecules are either moving away from the central propane or becoming more ordered.

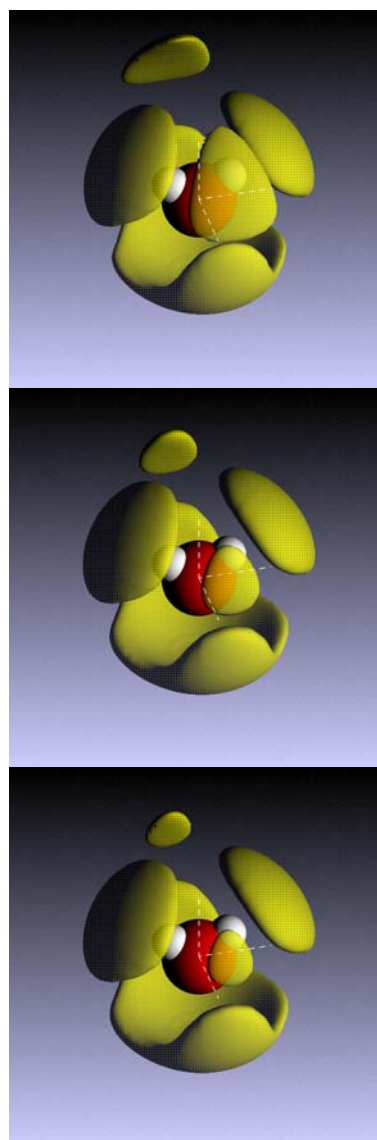


Figure 5. The spatial density functions at the 20% level for the three propane-water mixtures are varying degrees of propane hydrate formation: (a) 0%, (b) 6% and (c) 10%.

This expansion of the hydration structure is also observed when examining the propane-water correlations. These correlations may be divided into two groups the carbon-water correlations, namely, the $g_{COw}(r)$ and the $g_{CHw}(r)$ functions shown in figures 6a and 6b, respectively, and the $g_{MOw}(r)$ and $g_{MHw}(r)$ functions shown in 7a and 7b, respectively. In all these correlations there is a marked difference between the propane-water (0% formed) correlations and the part-formed correlations (6% and 10%). The propane-water mixtures in the presence of hydrate show a loss in peak sharpness and amplitude. Additionally, there is on average a 0.1-0.15Å increase in intermolecular distances from the correlation with no hydrate formed (0% formed) to the part-formed cases, highlighting the expanding structure as more propane hydrate forms.

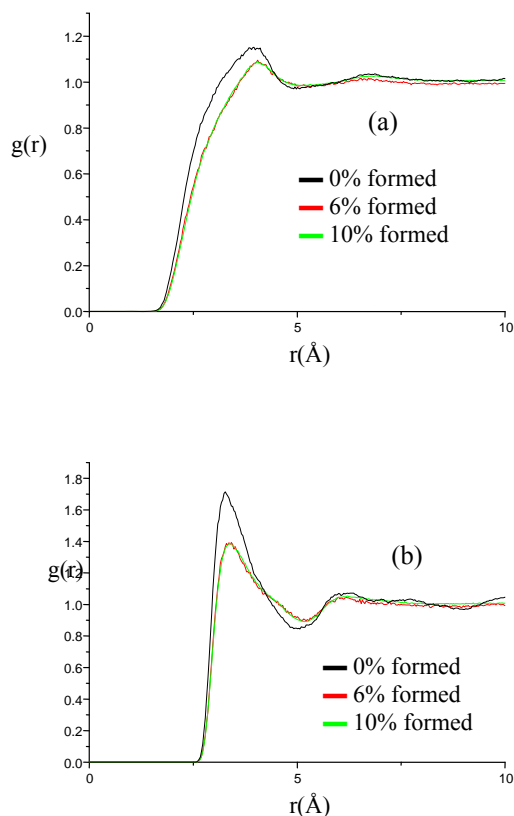


Figure 6. The carbon-water partial pair correlation functions: (a) $g_{COw}(r)$ and (b) $g_{CHw}(r)$ correlations determined by the EPSR procedure from the simulated propane-water model at 0% (black), 6% (red) and 10% (green) propane hydrate formation

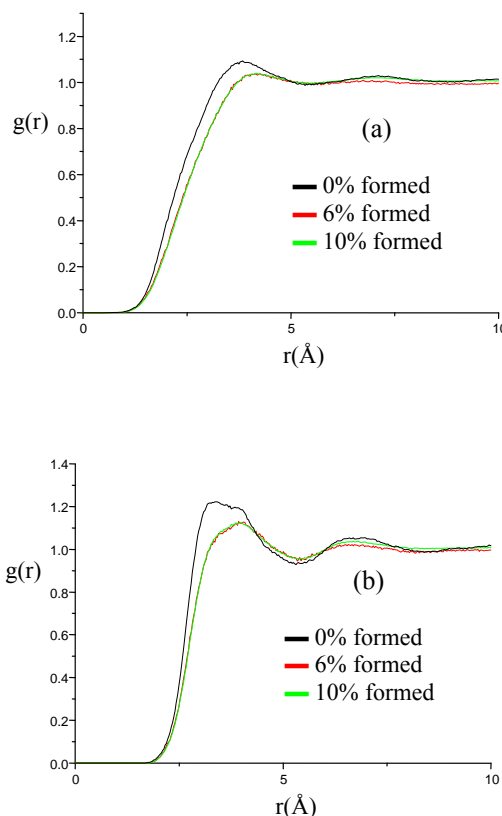


Figure 7. The propane-water partial pair correlation functions: (a) $g_{MOw}(r)$ and (b) $g_{MHw}(r)$ correlations determined by the EPSR procedure from the simulated propane-water model at 0% (black), 6% (red) and 10% (green) propane hydrate formation.

Propane Hydrate

The propane hydrate crystal radial distribution functions (figure 8) show a longer-range order than is observed in the propane-water liquid phases which also demonstrates that EPSR is able to analyze the crystal data and not just the amorphous stages. There are clear differences between the water-water correlations from the liquid phases (0%, 6% and 10%) and those obtained for the crystal. The correlations from the crystal show sharper and more pronounced peaks (figure 7) with large differences in peak amplitudes. It is clear that these peaks are largely preserved in position when compared to the liquid phases. The first peak in the $g_{OwOw}(r)$ of the propane hydrate crystal is centered at about 2.73Å which is in good agreement with the values from the part-formed data and the propane-water structure (0%). Similarly, the first peaks in the

$g_{OwHw}(r)$ and $g_{HwHw}(r)$ correlations are centered at about 1.79Å and 2.32Å, respectively, which are also in good agreement with the data from the liquid phases.

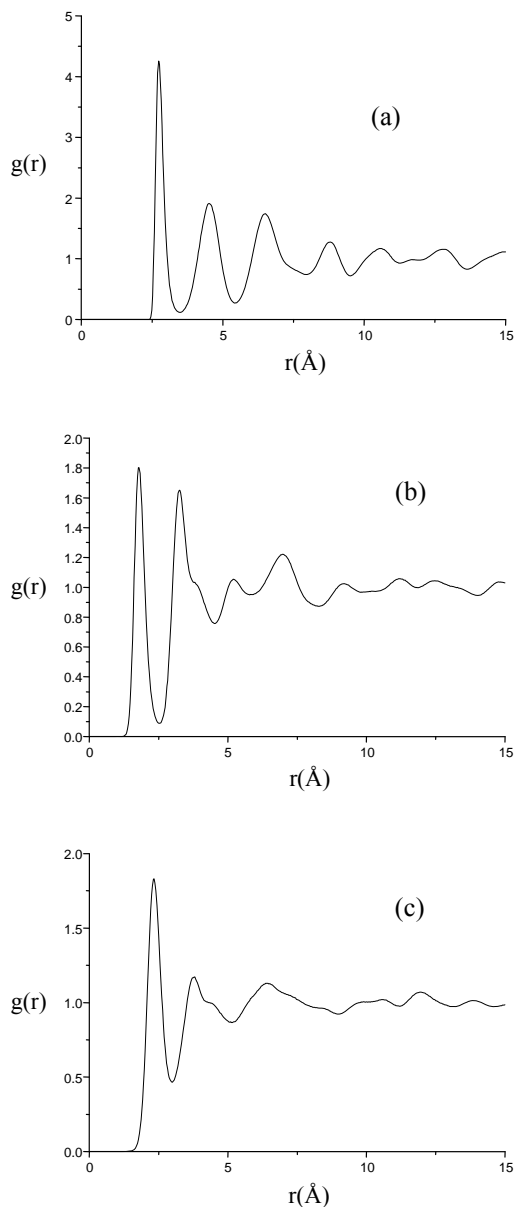


Figure 8. The water-water partial pair correlation functions: (a) $g_{OwOw}(r)$, (b) $g_{OwHw}(r)$, and (c) $g_{HwHw}(r)$ determined by the EPSR procedure from the simulated propane hydrate model

The $g_{COw}(r)$ plots exhibit a distance increase from 3.28Å in the propane-water (0%) to a distance of 4.22Å in the crystal (figure 9). The $g_{CHw}(r)$ correlation shows an increase from 3.94Å (at 0%) to 4.37Å in the crystal structure (figure 9). In a

similar way the first peak in the propyl hydrogen-water correlations, $g_{MOw}(r)$ and $g_{MHw}(r)$, show peaks which are centered at about 4.22Å and 3.95Å, respectively (figure 10). These peaks are approximately 0.5Å larger in the crystal than the propane-water liquid mixtures. This suggests that the large cage of the sII hydrate crystal is significantly larger than the solvation cage for propane in liquid water.

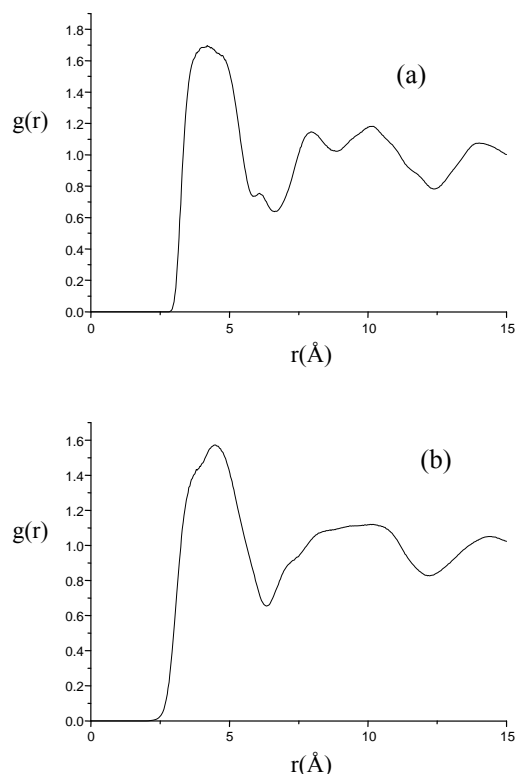


Figure 9. The carbon-water partial pair correlation functions: (a) $g_{COw}(r)$ and (b) $g_{CHw}(r)$ correlations determined by the EPSR procedure from the simulated propane hydrate model.

Propane-Water in the Presence of PVP Inhibitor

Figures 11 and 12 show the results obtained from measuring the propane-water structure without (i.e. the 0% formed data) and with PVP inhibitor.

The near perfect overlap between the samples with and without inhibitor shows no evidence of PVP significantly affecting the water structure of the propane-water system. A hypothesis proposed was that this inhibitor may operate by disrupting the water structure in a way that prevents water

molecules ‘coming together’ to form the hydrate cages and subsequently inhibit clathrate hydrate growth [10]. However, these neutron diffraction results indicate that the water structure appears to be identical with and without PVP in the propane-water mixtures at higher Q-values which represent intermediate-range order. It has been reported by a number of researchers that PVP inhibits hydrate growth as well as the hydrate nucleation period [1]. These results show there is no change in the first or second shell water structure.

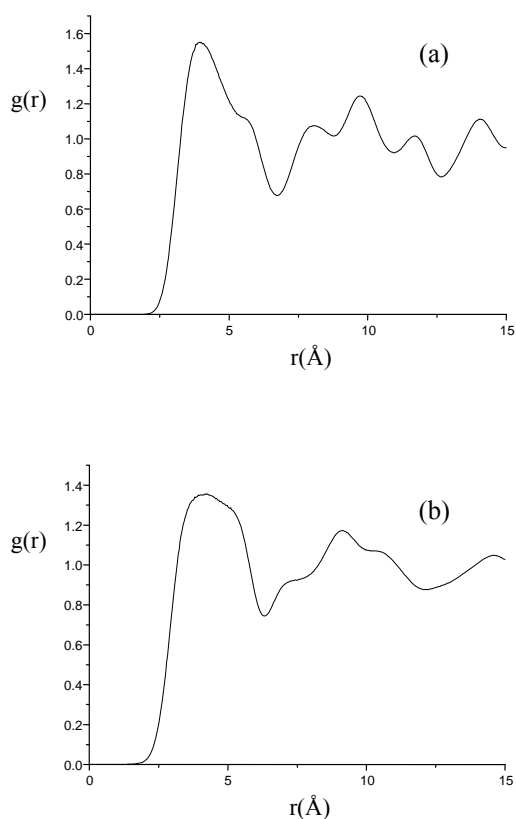


Figure 10. The propane-water partial pair correlation functions: (a) $g_{MOw}(r)$ and (b) $g_{MHw}(r)$ correlations determined by the EPSR procedure from the simulated propane hydrate model

TESTING THE EFFECT OF THE EPSR POTENTIAL

Different potential parameters and models were used to study the significance of these parameters. In this study, the site-site radial distribution functions for methane/water systems just below the clathrate hydrate formation boundary were estimated. The inputs to this structure refinement were the measured total structure factors as obtained from the neutron diffraction experiments

using (CD_4/D_2O) and (CH_4/D_2O), and the first order difference of these two data sets. Comparisons of the water structure determined by the SPC/E and TIP4P water models with Lennard-Jones methane using standard literature potential parameters highlighted the following main conclusions.

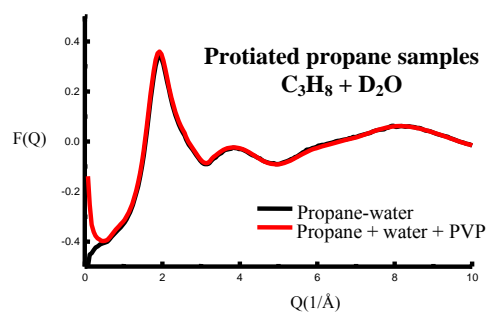


Figure 11. The total structure factor for the protiated propane-water mixture at 0% formation with and without 1 wt. % PVP, $C_3H_8 + D_2O + PVP$.

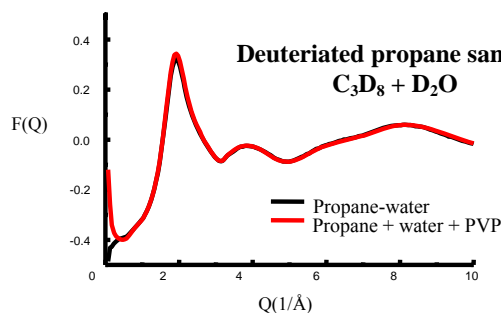


Figure 12. The total structure factor for the deuteriated propane-water mixture at 0% formation with and without 1 wt. % PVP, $C_3D_8 + D_2O + PVP$

By changing the potential parameters (σ and ϵ) of methane, not much difference was seen in the radial distribution functions. We have performed a number of tests to further validate the experimentally derived radial distribution functions obtained using EPSR. These tests were performed on the neutron diffraction data (isotopic substitution on water-hydrogen) measured for the water - methane system near the hydrate formation region (at 18 MPa and 291 K). Two sets of starting reference potentials were used in the EPSR simulations: SPC/E [11] and L-J [9] models and TIP4P [12] and L-J [9] models.

Figure 13 shows the hydrogen-hydrogen (a), hydrogen-oxygen (b), and oxygen-oxygen (c) radial distribution functions obtained using SPC/E and TIP4P references. These results indicate that the hydration shell structural results generated from EPSR computer simulations are not significantly sensitive to the reference starting potential.

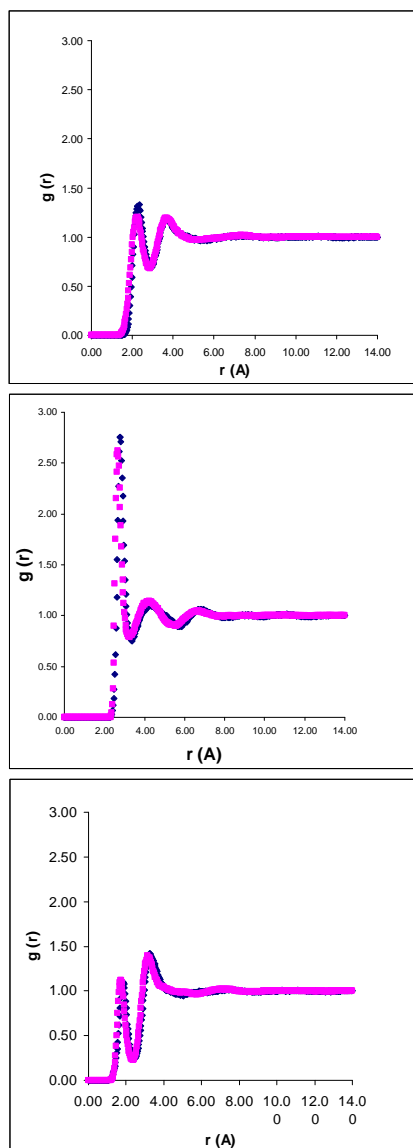


Figure 13. (a). H-H, (b). H-O_w and (c) O_w-O_w radial distribution functions for methane - water generated using SPC/E and TIP4P water reference models and the L-J model for methane.

CONCLUSIONS

From the combined neutron diffraction – EPSR computer simulation studies, the hydration structure was found to be different in the liquid

phases of the part-formed propane hydrate (sII type hydrate) compared to that before any hydrate formation. This effect was clearly demonstrated by the spatial density functions and also by interrogating the radial distribution functions that describe the propane – water interactions. Significant changes in these interactions were observed in going from the liquid propane-water mixture to propane hydrate. These radial distribution functions were obtained through the EPSR technique which has also been shown to be able to fit the crystal structure of sII hydrate.

The effect of adding 1 wt.% of a kinetic hydrate inhibitor, PVP, on the water structure was examined. The measured total structure factors from propane-water mixtures that contained PVP in the mixture showed no evidence of a change to intermediate-range water structure compared to the mixture with no PVP present.

Another conclusion that may be drawn from these results is that there was no evidence for the existence of any metastable phases during the formation of propane hydrate and methane hydrate.

ACKNOWLEDGEMENTS

The authors would like to thank the EPSRC and ISIS Facility for funding this work. Support from Chevron Technology Company is also acknowledged. Thanks also to John Dreyer and John Bones for their invaluable assistance during the experiments.

REFERENCES

- [1] Sloan, E.D., Koh, C.A., *Clathrate Hydrates of Natural Gases*, 3rd Ed., CRC Press, Boca Raton, FL, 2008.
- [2] Soper, A.K., Howells, W.S., Hannon, A.C. *ATLAS-Analysis of Time of Flight Diffraction Data from Liquids and Amorphous Samples*, Rutherford Appleton Laboratory, 2000.
- [3] Buchanan, P., Soper, A.K., Thompson, H., Westacott, R.E., Creek, J.L., Hobson, G., Koh, C.A., *J. Chem. Phys.*, 2005: 123: 164507.
- [4] Soper, A. K., *Mol. Phys.*, 2001: 99: 1503.
- [5] Bowron, D. T., Finney, J. L., Soper, A. K., *J. Phys. Chem. B*, 1998: 102: 3551.
- [6] Mak, T.C.W., McMullan, R. K., *J. Chem. Phys.*, 1965: 42: 2732.

- [7] Thompson, H., Soper, A.K., Buchanan, P., Aldiwan, N., Creek, J.L., Koh, C.A., J. Chem. Phys., 2006: 124: 164508
- [8] Jorgensen, W. L., Madura, L. D., Swenson, C. J., J. Am. Chem. Soc., 1984: 106: 6638.
- [9] Berendsen, H. J. C., Grigera, R. J., Straatsna, T. P., J. Phys. Chem., 1987: 91: 6269.
- [10] Sakaguchi, H., Ohmura, R., Mori, Y. H., Journal of Crystal Growth, 2003: 247: 631.
- [11] Berendsen, H. J. C., Grigera, R. J., Straatsna, T. P., J. Phys. Chem., 1987: 91: 6269.
- [12] Jorgensen, W.L., Chandrasekhar, J., Madura, J.D., Impey, R.W., Klein, M.L. J Chem Phys., 1983: 79: 926.